Photothermal imaging bundle system for estimating tissue oxygen saturation

Yonat Milstein[1], Dror M. Allon[2], James Harrington[3], Carlos Bledt[3] and Israel Gannot[1]

1. Dept. of Biomedical Optics, Tel Aviv University, Tel Aviv 69978, Israel 972-36406592

2. Dept. of Oral and Maxillofacial Surgery, Rabin Medical Center, Israel 972-393756458

3. Department of Material Science and Engineering, Rutgers University, Piscataway, NJ 08854

ABSTRACT

The objective of this study is to validate a method for the measurement of tissue oxygen saturation level via a thermal imaging bundle *in-vitro* and *in-vivo*. The method consists of a thermal imaging system and an algorithm which estimates the compound concentration according to the temperature rise of the tissue. A temperature rise is obtained by illuminating the tissue in the NIR range and is measured using a thermal camera and a coherent thermal imaging bundle for non-invasive transendoscopic use. The system was validated using agar phantoms of varying concentrations of Methylene Blue and ICG as well as blood samples. The algorithm estimated the Methylene Blue relative amount and the results were compared to the real relative amount. The calculated RMS of the error was 5.12%, a satisfying value for this stage. In the blood samples, for oxygenation levels higher than 50% the RMS of the error was 5.79%. Once the system was verified a portable system was built for clinical use, this system was also evaluated on agar phantoms and the RMS of the error was 10.64%. As a result of the encouraging experiments *in-vivo*, animal trials were performed. The oxygenation levels of mice were decreased and were estimated respectively using our system. The system determined a small decrease in the tissue oxygen saturation of the mice. These results verify the algorithm's and bundle's suitability for the use in a non-invasive system. They provide motivation for performing more complex *in-vitro* experiments and moving on to clinical trials.

Keywords: photothermal spectroscopy, tissue oxygen saturation, thermal imaging, coherent waveguide bundle, thermal imaging bundle.

1. INTRODUCTION

Oxygen saturation is a significant and important parameter of a biological tissue, indicating tissue vitality and functionality level. Malignant tumors are characterized by abnormal oxygen saturation values compared to their surroundings due to angiogenesis processes[1]. Measuring oxygen saturation is significant in many procedures, including tumor detection, cancer treatment adjustment and ischemia monitoring during medical procedures[1, 2]. Detecting the oxygen saturation level in an efficient non-invasive method can substantially improve the treatment in such cases. Accurate oxygenation measurements of a tissue can be used to indicate functional bioenergetic changes evaluation and therefore in cancer detection. Thus, an accurate oxygenation measurement of a tissue can be a potential tool for diagnosis of malignant lesions, particularly if being non-invasive. In spite of all the above, oxygen saturation level measurements have yet to become a common diagnostic tool for characterizing malignant tissues.

Photothermal spectroscopy was investigated thoroughly and used for numerous applications[3, 4]. The high sensitivity of the method to surface measurement is extremely valuable in cancer detection, since the majority of

Optical Fibers and Sensors for Medical Diagnostics and Treatment Applications XII, edited by Israel Gannot, Proc. of SPIE Vol. 8218, 82180D · © 2012 SPIE
CCC code: 1605-7422/12/$18 · doi: 10.1117/12.917008

cancers in humans arise from epithelial cells[5]. Although there are some implementations of saturation measurement methods for external use[6, 7] none of them utilizes the advantages of fiber bundles and photothermal spectroscopy for oxygen saturation imaging of internal tissues. The incorporation of a waveguide bundle in order to fit a system for non-invasive use and for cancer diagnosis in particular, has not been developed and researched. This will enable these measurements for transendoscopic use and advance the issue in discussion greatly since the existing methods cannot operate as an independent, non-invasive diagnostic apparatus. A coherent infrared bundle consisting of waveguides capable of transmitting IR radiation was developed[6, 8, 9]. The bundle enables imaging of saturation levels in a tissue using a thermal camera. A bundle with an optimal configuration for our use, in terms of waveguide diameter, length, and fabrication materials allows the transmission of a thermal image from a distant tissue to a thermal camera. This, in practice, adapts the system for a non-invasive procedure and allows the analysis of suspected internal cancer lesions. This combination will enable to measure small changes in internal tissue's oxygenation and therefore detect the cancerous region at an early stage. Detecting the oxygen saturation level in an efficient non-invasive method can substantially improve early detection and treatment. Adapting the system for transendoscopic use will enable non-invasive diagnosis of internal cancerous tissue..

Previous work by Tepper et. al[10] presented a minimal invasive method for saturation measurement. In this method a tissue is illuminated with several wavelengths, by a laser in the NIR range. Each wavelength is absorbed in the tissue, depending on its absorption coefficient, and causes a different temperature rise measured with an IR camera. By analyzing the temperature rise as a function of the illumination wavelength, the oxygen saturation level is determined using a curve fitting algorithm. The study presented a theoretical model and initial experiments verifying the method. Despite the encouraging results there was no validation of the method for internal minimal invasive use. At a later stage a bundle in the IR range[9, 11] was incorporated in the method for the development of a minimal invasive system.

2. METHODS

2.1 System validation

System validation was performed in two stages, first on agar phantoms and later on blood samples. The agar phantoms were comprised of two absorbers, Methylene Blue (MB) and ICG. These materials have different absorption spectra in the NIR range and may simulate the differences in the absorption of oxygenated and deoxygenated hemoglobin. Solutions of the two absorbers in various ratios were added to agar to create the different phantoms.

The samples were illuminated using a continuous-wave tunable titanium–sapphire laser. The illumination was performed in five wavelengths in the NIR range, 740, 755, 770, 785 and 805nm in order to acquire data of temperature change as a function of wavelength which the algorithm analyzed at the next stage. The temperature was measured using a thermal imaging camera (Thermovision A40; FLIR Systems) and the bundle. Three different bundle configurations were used in order to evaluate and determine the optimal one. The first bundle consisted of 19 Teflon fibers of 1.1mm diameter and a length of 15cm. The second consisted of 19 Silica fibers of 1mm diameter and a length of 17cm. The third consisted of 16 Silica fibers of 0.32mm diameter and a length of 20cm.

At the second stage blood sample experiments took place. The experiments were done using type B+ human blood and the oxygenation level of the blood was determined by adding Sodium dithionite (Sigma Aldrich, Israel) in varying concentrations ranging from 0.2 to 2.7 mg/g blood [12]. Five blood samples with oxygenation levels of 0.3%, 20%, 50%, 70%, 81% were tested. The samples were illuminated in the same way as the phantoms, the temperature change was measured and the oxygenation of the samples was estimated.

2.2 Portable system

Once the basic bundle system was validated and an optimal bundle configuration was chosen a portable system was developed. This portable system was used for measurements performed out of the lab. The portable system consisted of two elements, an illuminating element and an imaging element.

The illuminating element consists of a 150W white light source (OSL-1EC, Thorlabs), a filter wheel (FW102C, Thorlabs) with 5 filters. The filters are with center wavelengths of 700,730,790, 820 and 850 and FWHM of 10nm. A transmitting fiber with a 6.35mm diameter and 91cm long transmits the light to the tissue. Three plano convex lenses with 1" diameter and f=2.54mm are used for focusing purposes. The illuminating element replaces the laser in the laboratory system. The filters allow the transmittance of the relevant wavelengths while blocking the rest of the light spectrum. Using the motorized wheel enables fast and automatic filter change and by that the transmitted wavelength changes. The first plano convex lens is located between the light source output and the filter wheel for maximizing the light on the filter. The other two lenses are used for focusing the light exiting the filter in to the light guide who transmits the light to the distant tissue or sample. An image of the final illuminating element is presented in Figure 1(b).

The imaging element includes a small dimension thermal camera, (Tau-320, FLIR) a ZnSe plano convex lens, 1" diameter and f=3", for focusing and the fiber bundle. The Tau-320 camera is an uncooled camera, with a 9mm lens and a sensitivity of less than 50mK. The camera's dimensions are 44.5x44.5x30.0mm making it suitable for a small portable system. This element records the temperature change at the far end using a bundle which transmits the image to the camera. The image is processed using MATLAB. An image of the imaging element is shown in Figure 1(a)

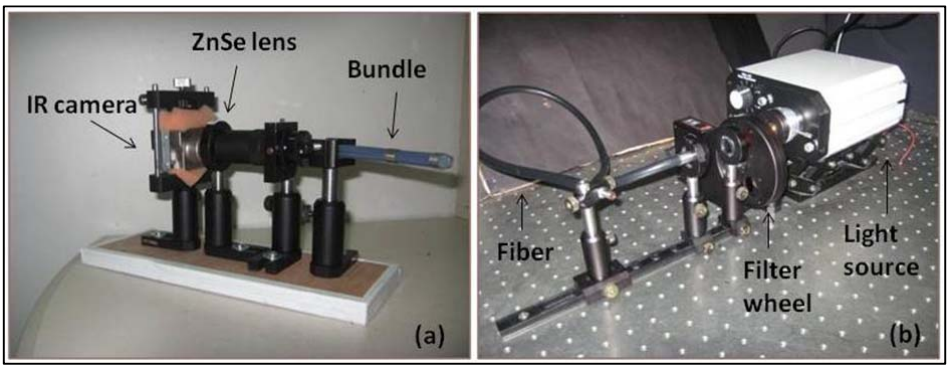

Figure 1: The portable system. The imaging element including the thermal camera, lens and bundle (a). The illumining element (b).

The entire portable system was validated using agar phantoms. Five agar phantoms comprising of MB and ICG were illuminated. The relative amount of the five phantoms was 0%, 25%, 50%, 75% and 100% of MB. Once the phantom relative amount was estimated the E_{RMS} of the system was found.

2.3 Animal trials

Animal trials were performed at Rabin Medical Center in collaboration with Dr Dror Allon from the Oral and Maxillofacial Surgery Department. The trials began following the approval from the council for animal experiments. The purpose of the trial is to evaluate the ability of the system as an oxygen saturation estimator. Using the method on a live animal will take into account all variables in regard to changes during philological changes of the animal. In order to evaluated the method the oxygen saturation of the blood must be varied in some way in order to create data for the measurements. This was chose to be done by changing the inhaled oxygen relative amount. The relationship between the different blood and pressure parameters are described in the Alveolar gas equation[13]:

$$P_AO_2 = F_IO_2\left(P_{ATM} - pH_2O\right) - \frac{p_aCO_2}{RQ} \quad (1)$$

The F_IO_2 values were chosen in order to create three physiological states, normoxia (PaO2>60mmHg), moderate hypoxia (45mmHg<PaO2<60mmHg) and sever hypoxia (PaO2<45mmHg)[14].

A measuring chamber was fabricated for the trial, the chamber was created out of plastic and was sealed. A gas mixture comprised of O_2 and N_2O flowed in to create the desired F_IO_2 for the animal. The imaging and an apparatus for positing the animal were placed inside the chamber while the illuminating element was placed out of the chamber. The imaging element was connected to a computer set out of the chamber for recording the data. Once the animal was placed in the measuring spot the measuring process took place in the same manner as in the validation experiments. Figure 2 shows the chamber with the different elements and the illumination process.

One group (n=12) of white ICR mice, (22-30g) was studied. The experiment was performed three times for each mouse with FIO2 values of 0.21, 0.15 and 0.10. For the 0.21 fraction the mice were placed in the air. For the 0.15 fraction the mice were placed in the sealed chamber and a gas mixture comprised of O_2 and N_2O flowed in with a rate of flow of 1l/min and 6 l/min respectively. For the 0.10 fraction the rate of flow was 1l/min and 9 l/min respectively. The measurements were performed using the portable system and the oxygen saturation was evaluated.

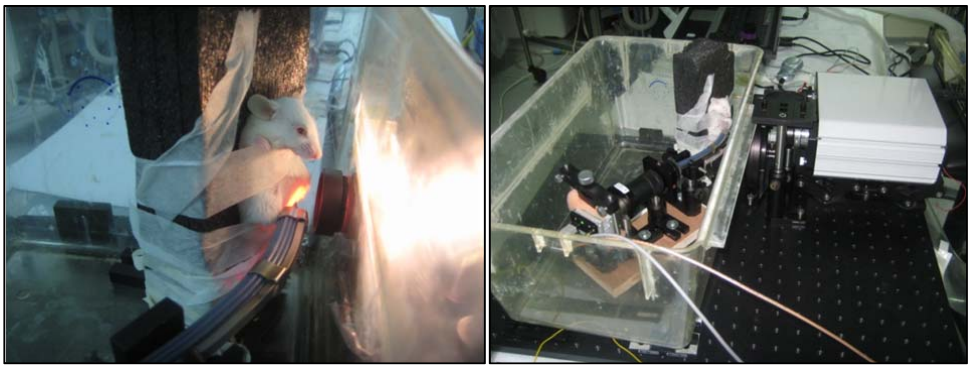

Figure 2: The animal trial experimental setup (Right), a mouse during the illumination process (Left)

3. RESULTS

3.1 System validation

For the agar phantoms, the algorithm estimated the relative amount of MB in each phantom. This was performed using the three described bundles. The estimation RMS of the error obtained for the three bundles were 5.12%, 7.55%, 17.39% respectively. Figure 3 presents the real relative amount of the phantoms vs. the estimated one. According to these results bundle no.1, consisting of Teflon fibers, was chosen as the optimal configuration and was used in the portable system.

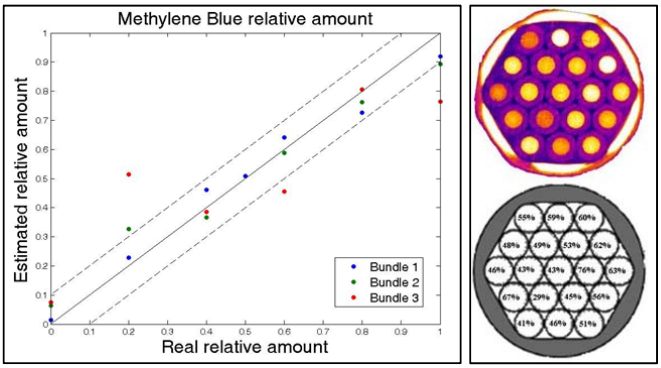

Figure 3: The real relative amount vs. the estimated relative amount for the three bundles (Left). The IR camera image and the estimated relative amount for the different fibers of the bundle (Right)

For the blood samples the algorithm estimated the samples oxygenation level of each sample. Samples with an oxygenation level higher than 50% were estimated with an averaged RMS of the Error of 10.16% for these levels [11]. The results are shown in Table 1.

Real oxygenation level	3%	20%	50%	70%	82%
Estimated oxygenation level	71%	60%	56%	62%	83%

Table 1: Blood experiments results, the real oxygenation level versus the estimated oxygenation level

3.2 Portable system

The portable system was validated by performing agar phantom experiments where the MB relative amount was estimated according to the temperature difference at the five wavelengths. The E_{RMS} obtained for the experiments was 10.64%. The results are presented in Figure 4. In addition the imaging element was evaluated in order to find the system's specifications. The temperature resolution was found to be $0.13^{O}C$, the noise equivalent temperature difference was $0.1^{O}C$ and the spatial resolution was 1.05 [Lines/mm].

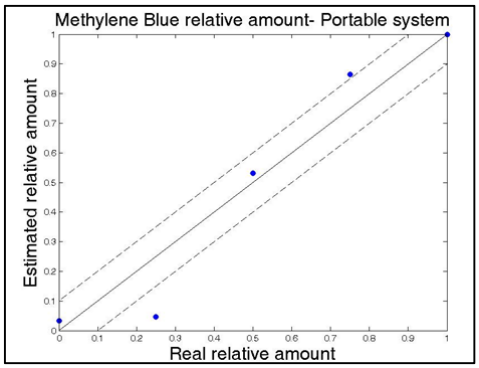

Figure 4: The MB estimated relative amount using the portable system versus the real relative amount.

3.3 Animal trials

The animal trials were performed as mention in section 2.3. During the 0.15 fraction experiment one mouse died and during the 0.10 fraction experiment two mice died. Therefore the results for these two experiments represent 11 and 9 subjects respectively. The results are displayed in Table 2, showing the evaluated tissue oxygen saturation compared to the calculated arterial oxygen saturation based on equation (1).

	Normoxia	Moderate hypoxia	Severe hypoxia
F_IO_2	0.21	0.15	0.1
Calculated Arterial SO_2	97.56%	87.88%	28.8%
Evaluated tissue SO_2	81.40%±5.9	80.90%±5.2	78.30%±6

Table 2: Animal trial results, evaluated tissue oxygen saturation

The results of this trial show that the system was able to detect the expected decrease in the tissue oxygen saturation. Despite that, the decrease is not extreme as in the arterial oxygen saturation. The reason in the difference of the two could be a slower process in the change of a tissue oxygen saturation compared to that of the arterial blood which seems to be a rapid process. Another option could be limitations of the system in evaluating the exact tissue oxygen saturation *in-vivo*. Due to that, more experiments are needed in order to determine the exact abilities and accuracy of the system for evaluating the tissue oxygen saturation *in-vivo*.

4. CONCLUSIONS

A base for a non-invasive system for photothermal oxygen saturation measurements was presented. The incorporation of a coherent waveguide bundle allows measurement of the oxygenation within cavities. The material relative amount measurements could be used for oxygenation measurements. These can be utilized to detect cancerous regions in the tissue and therefore improve cancer detection rates and treatment. The system was validated successfully and the portable system was designed and built. An optimal apparatus was desired and for that reason the design was based on bundle evaluation tests as well as analyzing all apparatus elements. This provided the first portable system for the *in-vivo* tests. Initial *in-vivo* experiments took place, yet more complex ones are needed in order to find the accuracy and abilities of the system *in-vivo*. The main advantage of the proposed method is its ability to measure in a non-invasive way the oxygen saturation of a suspected tissue.

5. ACKNOWLEDGMENTS

We thank the US-Israel BiNational Foundation for their support through grant no.: 2007382. We thank the Israeli cancer association for their support through grant no. 20100050. We thank Slezak Foundation for their support through grant no. 32003194000.

6. REFERNCES

1. Brizel, D.M., S.P. Scully, J.M. Harrelson, L.J. Layfield, J.M. Bean, L.R. Prosnitz, and M.W. Dewhirst, *Tumor oxygenation predicts for the likelihood of distant metastases in human soft tissue sarcoma.* Cancer research, 1996. **56**(5): p. 941.
2. Kondepati, V.R., H.M. Heise, and J. Backhaus, Recent applications of near-infrared spectroscopy in cancer diagnosis and therapy. Analytical and Bioanalytical Chemistry, 2008. 390(1): p. 125-139.
3. Milner, T.E., D.M. Goodman, B.S. Tanenbaum, and J.S. Nelson, Depth profiling of laser-heated chromophores in biological tissues by pulsed photothermal radiometry. Journal of the Optical Society of America A, 1995. 12(7): p. 1479-1488.
4. Jacques, S.L., J.S. Nelson, W.H. Wright, and T.E. Milner, Pulsed photothermal radiometry of port-wine-stain lesions. Applied optics, 1993. 32(13): p. 2439-2446.
5. Jemal, A., R. Siegel, E. Ward, Y. Hao, J. Xu, T. Murray, and M.J. Thun, Cancer Statistics, 2008. CA Cancer J Clin, 2008. 58(2): p. 71-96.
6. Gopal, V., J.A. Harrington, A. Goren, and I. Gannot, Coherent hollow-core waveguide bundles for infrared imaging. Optical Engineering, 2004. 43: p. 1195.
7. Tremper, K.K., Pulse oximetry. Chest, 1989. 95(4): p. 713.
8. Gal, U., J. Harrington, M. Ben-David, C. Bledt, N. Syzonenko, and I. Gannot, Coherent hollow-core waveguide bundles for thermal imaging. Applied Optics, 2010. 49(25): p. 4700-4709.

9. Gannot, I., Thermal imaging bundle- A potential tool to enhance minimally invasive medical procedures. IEEE Circuits and Devices Magazine, 2006. 21(6): p. 28-33.
10. Tepper, M., R. Neeman, Y. Milstein, M.B. David, and I. Gannot, Thermal imaging method for estimating oxygen saturation. Journal of Biomedical Optics, 2009. 14: p. 054048.
11. Milstein, Y., M. Tepper, M.B. David, J.A. Harrington, and I. Gannot, Photothermal bundle measurement of phantoms and blood as a proof of concept for oxygenation saturation measurement. Journal of Biophotonics, 2010.
12. Briely-S b, K. and A. Bj rnerud. Accurate de-oxygenation of ex vivo whole blood using sodium dithionite. 2000.
13. Curran-Everett, D., A classic learning opportunity from Fenn, Rahn, and Otis (1946): the alveolar gas equation. Advances in physiology education, 2006. 30(2): p. 58.
14. Julien, C., A. Bradu, R. Sablong, E. Grillon, C. Remy, J. Derouard, and J. Payen, Measuring Hemoglobin Oxygen Saturation During Graded Hypoxic Hypoxia in Rat Striatum. Anesthesia & Analgesia, 2006. 102(2): p. 565-570.